

PREPARATION AND NOISE ANALYSIS OF POLYMER GRAPHITE CATHODE

Alexandr Knápek¹⁾, Miroslav Horáček¹⁾, Jana Chlumská¹⁾, Tomáš Kuparowitz²⁾,
Dinara Sobola²⁾, Josef Šikula²⁾

1) Institute of Scientific Instruments of the Czech Academy of Sciences, v. v. i., Královopolská 147, 612 64 Brno, Czech Republic (✉ knapek@isibrno.cz, 420 541 514 258, mih@isibrno.cz, jana.chlumaska@isibrno.cz)

2) Brno University of Technology, Faculty of Electrical Engineering and Communication, Technická 8, 616 00, Brno, Czech Republic (xkupar01@stud.feec.vutbr.cz, sobola@vutbr.cz, josef.sikula@ceitec.vutbr.cz)

Abstract

The paper deals with the preparation and measurement of an experimental polymer graphite cathode that seems to be a promising and cheap source of electrons utilizing cold field-emission in high- and ultra-high vacuum. Polymer graphite seems to be a proper material as it contains a large amount of hybridized carbon with a low degree of surface oxidation and *silicon monoxide* (SiO). Within the frame of this work, a special experimental method of tip preparation has been designed and tuned. This method is based on ion milling inside a dual-beam electron microscope enabling to obtain ultra-sharp tips of a diameter smaller than 100 nm with a predefined opening angle. The charge transport within experimental samples is evaluated based on results provided by the noise spectroscopy of the total emission current in the time and frequency domains.

Keywords: field emission, polymer graphite, noise analysis.

© 2018 Polish Academy of Sciences. All rights reserved

1. Introduction

Cathodes based on a pure field emission operating at room temperature (~ 300 K) are generally desirable for employing in electron optical devices working with a focused beam of electrons. As for pros, the most important include: high brightness (10^{13} A/m²sr), high current density (10^{10} A/m²), a small source size (< 0.01 μ m), a high spatial coherence, and, last but not least, their small energy spread. As for cons, the most problematic seems now the stability of the total emission current which is negatively influenced by the tip cleanliness [1]. Since the tip is operated at room temperature, the active area of the emission is not being simultaneously cleansed by the effect of heating as it is known from thermally stimulated cathodes operating at high temperature (~ 2700 K). Contaminants which are present on the tip surface locally affect work function causing inhomogeneity of the quantum barrier affecting field emission performance in time [1]. Even though there are several papers describing certain stabilization using a controllable resistor in the high-voltage loop between the control electrode and the cathode [2], a physical solution for this issue has not been yet presented.

Carbon has recently been considered one of the essential elements in the latest attempts to create a stable, long-life and sufficiently bright source of free electrons. Carbon allotropes that are mostly used for field emission related experiments are *carbon nanotubes* (CNT), graphene

and *highly ordered pyrolytic graphite* (HOPG). However, various kinds of graphite seem to be interesting for field emission experiments as well [3–5]. For our experiments, we have picked a special composite material based on graphite, the so called “polymer graphite”, as mentioned before. The polymer graphite is easily disposable and provides high amount of sp^3 hybridized carbon (approx. 80%). This kind of graphite is mostly used as a pencil lead for modern micro pencils of various diameters (usually 0.3–0.8 mm). Our “polymer”-branded mechanical pencil lead is of a 0.3 mm diameter. Comparing with the classic wood-case lead pencil graphite containing a mixture of graphite and clay to provide desired hardness, the mechanical pencil leads contain a very resilient and elastic non-ceramic bonding which is achieved by a high-temperature carbonization of the graphite with high polymers of natural origin in an oxygen-free environment. Although there is a growing interest in polymer graphite as an electrode material for electroanalysis due to its high electron transfer rates [6], there is still no paper presenting this material as a cathode emitting free electrons into the vacuum.

2. Experimental

In the first part of this section, a method of preparation which is based on focused-ion beam milling is presented. The second part deals with the measurement set-up and electrical characterization of the tips. In the last part, noise measurements take place presenting the main physical sources of the current beam fluctuations.

2.1. Preparing ultra-sharp tip

An adequately small ultra-sharp tip with a diameter lower than 100 nm is required for obtaining a sufficiently large electric field that is additionally amplified by a field-enhancement factor. The field-enhancement factor depends on the radius of curvature which sets the equipotential surfaces and so the electric field, which corresponds to the gradient of the potential. As for the tip geometry: even though it is possible to form lead pencil graphite by means of precise electrochemical etching [7], it is still not possible to obtain a desired surface tension which would form the required taper angle and a sufficiently small tip diameter. For this reason, a method incorporating a *focused ion-beam* (FIB) was devised and implemented within a dual-beam electron microscope FEI Helios NanoLab 660 enabling to prepare nanostructures of a high lateral and axial resolution. The basic preparation steps are illustrated in Fig. 1.

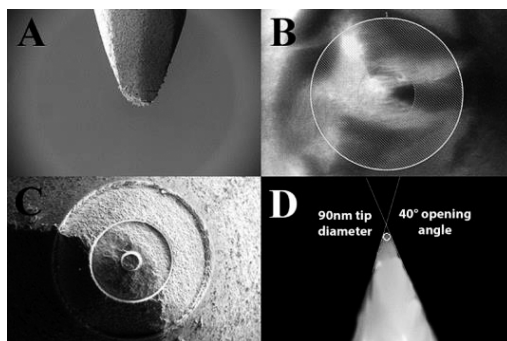


Fig. 1. Preparation of a sharp pencil lead tip by FIB: an SEM image of the preliminary shaped tip achieved by sanding (a); A view from above of the preliminary shaped tip with patterning (b); an FIB image of the stub with decreasing radius of the tip (c); an SEM image of the tip after final FIB milling (d).

An advantage of this approach is mainly the possibility of using the mechanically treated pencil lead which helps to avoid the use of chemicals and surface contamination in comparison with chemical wet etching. Hence, the preparation of a tip consists of two main steps: 1) sharpening mechanically the lead pencil graphite using sanding, and 2) FIB milling of the tip. To ensure the tip quality control, a high-resolution SEM is used to watch the tip geometry. A preliminary sharpened stub (Fig. 1a) is inserted into a microscope vacuum chamber, followed by FIB milling which is done in a circular pattern directly at the tip end (Fig. 1b). The first patterning is carried out using a high FIB current (65 nA), followed by another patterning where the FIB current decreases (Fig. 1c). By choosing accurate milling currents and pattern sizes (the inner and the outer diameters), it is possible to control the shape of the tip. It is also possible to prepare a tip of any shape and sharpness. The result of the FIB process is a sharp tip with sizes smaller than 100 nm. This 3D surface modification of a lead pencil graphite rod is shown in Fig. 1d.

2.2. Measurement set-up

The measurement set-up used (Fig. 2) is based on a previous set-up presented in the papers [1, 7]. A field emission cathode is placed in an extractor electrode embedded in a vacuum chamber ($P \sim 10^{-7}$ Pa) aiming towards an anode which accelerates electrons by a high voltage (5 keV). The accelerated electrons are collected on the scintillator electrode made of Cerium-doped *Yttrium Aluminium Garnet* (YAG) coated with a conductive layer, which enables to display an emission pattern, and also to measure a particular number of electrons caught by the conductive layer (approx. 10%).

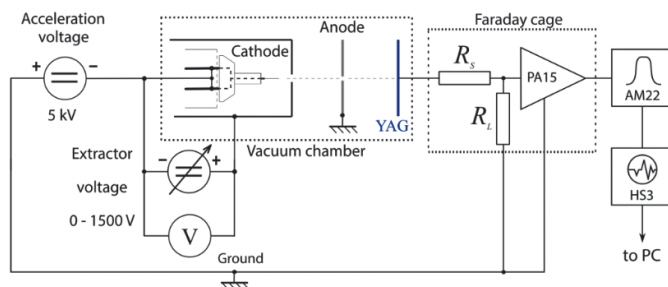


Fig. 2. The noise measurement set-up showing the connection of the electron gun and the noise measurement system located in a Faraday cage. A distance between the tip and the extraction cathode is usually 0.75–1 mm.

The measurement part of the set-up is placed outside the vacuum chamber in a Faraday cage shielding the measurement resistors R_S (491 k Ω), R_L (492 k Ω) and the preamplifier PA15 (20 dB) made by 3S Sedlak. The measurement amplifier AM22 is dynamically set based on the output signal level. The AM22 also serves as a filter providing a proper signal for the HS3 oscilloscopic card which samples the signal to the computer. Fig. 3 shows classical current-voltage characteristics based on the *Fowler–Nordheim* (FN) plot of the total emission current. It can be seen that the electron emission is based on the Fowler–Nordheim tunnelling process. The emission origin is thus considered to be caused predominantly by the field emission. A threshold of the applied voltage for the emission was above 240 V, usually up to 280 V, where the total emission current measured on a scintillator increases from 1 to 10 nA.

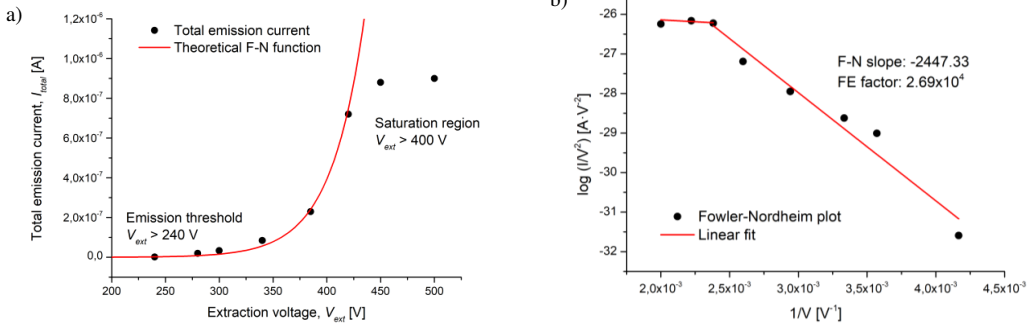


Fig. 3. The dependence of the total emission current (I_{total}) of graphite nanotip on the applied extraction voltage (V_{ext}) (a); the $\log(I/V^2)$ vs $1/V$ plot is shown: the black spots show the experimental data, and the red solid curves are the simulation results according to the FN equation (b).

2.3. Noise measurements

The current that is measured on the YAG scintillator in the time domain is transformed into the spectral domain and further analysed. It should be emphasized that the total emission current is lowered because of the collection efficiency of the YAG (approx. 10% of electrons are collected) and also because of the voltage divider which additionally lowers the current. An additional decrease of the signal intensity is due to the used resistor configuration, where only one half of the overall voltage is measured and therefore the obtained spectrum is decreased four times. Power spectral density is obtained by measuring particular frequency bands. Each band is determined by input and output cut-off frequency filters contained within the AM22 amplifier, which divides the spectrum into five parts. To avoid distortion caused by the filter characteristic, only a part of a spectral band is used, as it can be seen in Table 1. Before each measurement, the setup underwent an automated spectral calibration to achieve flat spectral sensitivity. The noise level of the inherent (background) noise of our setup, when shortened, equals $5 \times 10^{-17} \text{ V}^2/\text{s}$, which is low enough to measure even the thermal noise level. Each measurement took 480 seconds and during this period 80,000 samples were recorded. In pursuance of meeting the signal quasi-stationarity requirement for power spectral density analysis, the ideal sampling time of a single run $t = f_s \times N = 80 \times 103 \times 33.5 \times 106 = 418 \text{ s}$ has been empirically found. To reach a good frequency resolution at low frequencies, the sampled signal is processed by the *digital quadrature filter bank* (DQFB) of order $M = 4$, derived from the wavelet transformation algorithm.

Table 1. Bandwidths used to create the final spectrum.

Bands defined by filters	Frequency bands used
0.03 Hz – 300 Hz	0.1 Hz – 100 Hz
30 Hz – 3 kHz	100 Hz – 1 kHz
300 Hz – 30 kHz	1 kHz – 10 kHz
3 kHz – 300 kHz	10 kHz – 100 kHz
30 kHz – ...	100 kHz – 1 MHz

More detailed information about measurements of the low frequency noise and a description of particular problems that may be associated with such measurements is presented in [8]. In our measurement, the output of DQFB is a set of 16 band-limited fractional signals, where for

each sequence a fractional spectrum S_{yy} , evaluated by the Short-Time Discrete Fourier Transformation, is received. The resulting Power Spectral Density is calculated by the non-parametric Welch's method [1].

The results of noise measurements were obtained using two different extraction voltages representing two determined states of the field emission illustrated in Fig. 4 ($V_{ext} = 325$ V) and Fig. 5 ($V_{ext} = 525$ V). According to Fig. 3 (left), it can be seen that each voltage represents a different operation mode. For $V_{ext} = 325$, our cathode operates in a regular, unsaturated state and for $V_{ext} = 525$ V, the cathode operates in a saturation state, which means that for the increased extraction voltage the emission current does not increase anymore. For both extraction voltages, the thermal noise level is calculated, and its value is given by $4kTR$, where T is temperature, R is resistance and k is the Boltzmann constant [9]. For our measurement, $4kTR$ equals 4.07×10^{-15} V²/s (or V²/Hz).

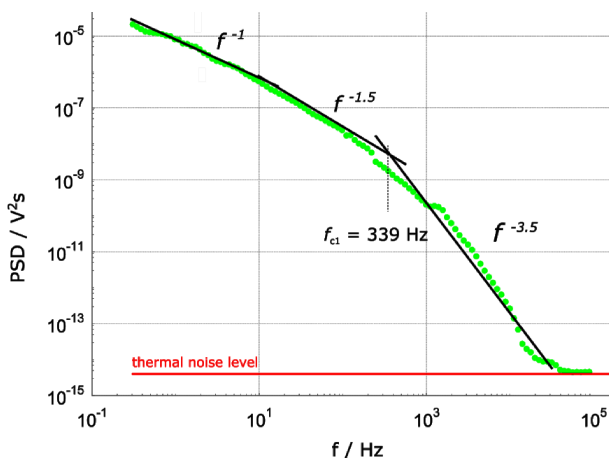


Fig. 4. Noise power spectral density for the total emission current measured at $V_{ext} = 325$ V at constant pressure and electron energy values. Plot colours are described in Table 1.

For $V_{ext} = 325$ V (Fig. 4), the $1/f$ noise which is also referred to as the “flickering” noise, dominates up to the cut-off frequency $f_{c1} = 339$ Hz. The $1/f$ noise is a process with such a frequency spectrum that the power spectral density is proportional to the reciprocal of the frequency and has been already studied in numerous papers [9–12]. As for the lower part of the spectrum where the $1/f^n$ noise is measured, the n parameter value is in a range $1.0 \leq n \leq 1.5$. The exact value of n is determined by the nature of recombination, the lifetime probability density function, and also by the trap density function. It has been already shown that the trap densities close to the conduction and valence band lead to higher values of n [13]. The cutting frequency is located near the region where the spectrum becomes steeper, which is caused by the superposition of particular $1/f$ and *generation-recombination* (G-R) processes. Such an effect may be explained by adsorption and desorption of various atoms present with some residual gas in the vacuum chamber, which happens on the tip surface. A precise model of adsorption-desorption has been formulated based on the Kolmogorov equation by Sergeev [14].

In the bulk, the volume diffusion (*i.e.* a diffusion within a single graphite flake) plays a more significant role, especially in the close vicinity of the emission tip, where temperature is increased due to electron tunnelling. For $V_{ext} = 525$ V, the spectrum slope shows such an influence, which is probably caused by increased temperature induced by a higher emission current. The diffusion

again takes place along with the *generation-recombination* process (G-R) caused by particle movement in the bulk towards the tip. The defects contained in the bulk – which are probably the “polymer” particles – behave like particle traps with an exponential energy distribution function. There are several cut-off frequencies associated with particular generation-recombination noise components; in particular: 8 Hz, 40 Hz, and 2 kHz.

Based on the presented data, our very first measurements show that the “polymer” pencil graphite may be used as a material for preparation of field emission cathodes when operating in a particular voltage regime. As for the setbacks which still prevent the cathode from working in a noiseless regime, it has been shown that the bulk defects, which are mostly cracks and inhomogeneity caused probably by the presence of higher polymers, behave like particle traps creating significant generation-recombination noise and hence the volume and surface diffusion which directly affects the number of emitted electrons. The correlation between the generation-recombination noise and the particle trapping/releasing was described in detail in our previous paper [1].

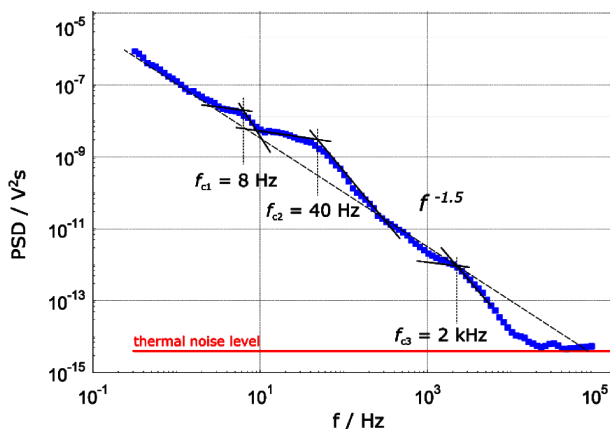


Fig. 5. Noise power spectral density for the total emission current measured at $V_{ext} = 525$ V at constant pressure and electron energy values. Plot colours are described in Table 1.

3. Results and discussion

3.1. Tip preparation using FIB milling

The classical approach to tip preparation is mostly based on electrochemical etching [7]. Since the surface tension is not constant in time as the tip elongates during the etching, it is not possible to prepare the tip with a predefined opening angle. FIB techniques do not suffer such setbacks. The local surface modification in combination with the topography control in nanoscale make this method reliable for preparation of tips from a cheap material source. For applications, where the surface cleanliness is not critical, the classical electrolytic etching [7] may be used instead of FIB.

3.2. Noise analysis

The total emission current measured on the YAG scintillator was further sampled and converted into a power spectrum density that has been subsequently worked with. Particular noise

components were determined in the obtained spectra based on different slopes of the fitting lines. Based on the present noise components, the charge transport in the bulk and at the tip of the cathode is described. The thermal noise component was neglected because of its low magnitude in comparison with the $1/f$ noise and G-R noise components which dominate the spectrum. For our case, the generation-recombination noise seems to be the most important factor influencing current stability: in the bulk of the cathode, the g-r noise originates from the particle movement in the bulk which is affected by structural inhomogeneity and defects contained in the bulk which were also reported by Navratil [6] who performed structural analysis of different “polymer“-branded leads. At the cathode tip, the G-R component is increased due to the electron attraction and release near the cathode surface, which is described in a previous paper [1]. The total emission current value is also decreased by the tip sputtering which continuously removes graphite flakes from the tip and hence blunts it. This results in discontinuous decreases in the total emission current. This phenomenon will be described in more detail in a separate paper.

4. Summary and conclusions

Noise measurements were performed on an entirely new polymer graphite cathode prepared by means of FIB in a dual-beam electron microscope, describing the charge transport and current stability of the total emission current showing the effect of bulk contaminants. Nevertheless, comparing this cathode with common metal FE cathodes, carbon exhibits many advantages; among them a low chemisorption rate of the CO and H₂ on a carbon surface compared with a metal surface. Another benefit that may make the cathode suitable for the use in focused electron beam devices is the fact that the extraction voltage can be kept low and thus limit the bombardment rate of the residual ions. To determine a specific application that should take advantage of the polymer graphite cathodes, the emitted *electron energy distribution spectra* (EEED) should be obtained in future.

Acknowledgements

This work was supported by EC and MEYS CR (project no. CZ.1.05/2.1.00/01.0017), and by the Technology Agency of the Czech Republic project no. TE01020118. This research was also subsidized by the Ministry of Education, Youth and Sports of the Czech Republic under the project CEITEC 2020 (LQ1601) and by the National Sustainability Program under the grant LO1401.

The authors would also like to thank Mr. Král, Mr. Hrubý and Mr. Sýkora for their support and assistance in the design of electrical and mechanical parts of the set-up.

References

- [1] Knápek, A., *et al.* (2012). Cold field-emission cathode noise analysis. *Metrol. Meas. Syst.*, 19(4), 417–422.
- [2] Harle, R. (1978). *Method for controlling the emission current of an electron source and an electron source having a control circuit for controlling the emission current.* U.S. Patent No 5, 808, 425.
- [3] Houdellier, F., *et al.* (2012). New carbon cone nanotip for use in a highly coherent cold field emission electron microscope. *Carbon*, 50(5), 2037–2044.

- [4] Khairnar, R.S., Dharmadhikari, C.V., Joag, D.S. (1989). Pencil lead tips: A field ion and field electron emission microscopic study. *Journal of Applied Physics*, 65(12), 4735–4738.
- [5] Knápek, A., et al. (2017). Field emission from the surface of highly ordered pyrolytic graphite. *Applied Surface Science*, 395, 157–161.
- [6] Navrátil, R., et al. (2016). Polymer lead pencil graphite as electrode material: Voltammetric, XPS and Raman study. *Journal of Electroanalytical Chemistry*, 783, 152–160.
- [7] Knápek, A., et al. (2017). Programmable set-up for electrochemical preparation of STM tips and ultra-sharp field emission cathodes. *Microelectronic Engineering*, 173, 42–47.
- [8] Kiwilszo, M., Smulko, J. (2009). Pitting corrosion characterization by electrochemical noise measurements on asymmetric electrodes. *Journal of Solid State Electrochemistry*, 13(11), 1681–1686.
- [9] Šikula, J., Levinshtein, M. (2004). *Advanced experimental methods for noise research in nanoscale electronic devices*. Boston: Kluwer Academic Publishers, 271–278.
- [10] Šikula, J., et al. (2007). RTS and $1/f$ Noise in Submicron MOSFETs. *AIP Conference Proceedings*, 71–76.
- [11] Šikula, J., et al. (2007). Quantum $1/f$ Noise in Bio-Chemical Resonant ZnO Sensors. *AIP Conference Proceedings*, 339–342.
- [12] Šikula, J., et al. (2003). Noise and non-linearity as reliability indicators of electronic devices. *Informacije Midem-Ljubljana*, 33(4), 213–221.
- [13] Mohammadi, S., Pavlidis, D. (2000). A Nonfundamental Theory of Low-Frequency Noise in Semiconductor Devices. *IEEE Transactions on Electron Devices*, 47(11), 2009–2017.
- [14] Sergeev, E., et al. (2013). Noise diagnostic method of experimental cold field-emission cathodes. *Noise and Fluctuations (ICNF), 2013 22nd International Conference IEEE*, 1–4.